Numerical Methods for a Population-Balance Model of a Periodic Fermentation Process

Francois B. Godin, David G. Cooper, and Alejandro D. Rey
Dept. of Chemical Engineering, McGill University, Montreal, Quebec, Canada, H3A 2B2

Population-balance models are often used in order to study systems that involve the breakup and agglomeration of discrete particles. Particulate systems, crystallization in solutions, and microbial systems are examples of where these types of models can be formulated (Ramkrishna, 1985). However, their use to simulate real processes is limited due to the complexity in obtaining accurate solutions. The solution to these models can sometimes be simplified by making certain assumptions; unfortunately, these assumptions are not always valid when simulating real systems.

In this communication, a robust, adaptive solution scheme is developed and used to solve a population-balance model applied to a real microbial process. This model was formulated to simulate a fermentation process known as self-cycling fermentation (SCF) (Brown and Cooper, 1991, 1992; Hughes and Cooper, 1996; McCaffrey and Cooper, 1995; Sarkis and Cooper, 1994; Sheppard and Cooper, 1990a,b; van Walsum and Cooper, 1993; Wentworth and Cooper, 1996; Zenaitis and Cooper, 1994). Although this work discusses a numerical scheme applied to the SCF process, it is intended to show that this method can be applied to other systems where population balance equations arise in modeling.

SCF is a fermentation technique in which synchronized cell cultures are obtained by periodically removing half of the reactor volume and replacing it with fresh medium (cycling). The periodicity of the system is induced by monitoring a growth-associated parameter, and allowing the system to cycle when an extremum in this parameter is detected. The periodicity of the system is not predetermined but develops due to a computerized feedback control. The results are that the organisms double exactly once during each cycle, in a synchronized fashion.

Cell-mass population-balance models for chemostat and batch systems have been solved successfully by Subramanian and Ramkrishna (Ramkrishna, 1971; Subramanian and Ramkrishna, 1971) by applying the method of weighed residuals using global basis functions. However in these simulations, the cell-mass distributions are relatively broad and evenly distributed in cell-mass space. In the case of SCF, synchronized cultures evolve and the cell-mass distributions are narrower in cell-mass space. When modeling such cultures, the solution to the population balance model must be obtained for cell-mass distributions that progress in time as fronts. The numerical scheme must be able to capture these sharp profiles without excessive oscillations in the solution. These sharp features can be very difficult to capture using global basis functions without having numerical oscillations in the solution. These oscillations can sometimes be overcome by increasing the number of global basis functions used. Unfortunately using a large number of basis functions greatly increases computing time. In addition, ill-conditioned matrices can arise under these conditions (Fletcher, 1984).

Adding to the complexity in obtaining a solution to the SCF model is the control of cycling in this fermentation method. The nearly instantaneous emptying and filling of the reactor results in temporal discontinuities in the cell-mass distribution and other growth trends. These temporal discontinuities are also inherent in other fermentation processes such as fed-batch and sequential-batch fermentations. To capture these trends with accuracy, the time steps used in the computations must be reduced to values much smaller than the time scale associated with these sharp trends. On the other hand, for intracycle features such as lags in growth curves, the time steps should not be reduced and thus increase computation time. In other words, an adaptive time scheme must be used.

Liou et al. (1997) described a method to obtain the solution of cell-mass population-balance models based on a successive generation approach. In their work, they assumed a constant growth environment and therefore did not couple a substrate balance with the population balance equation, which is necessary when modeling the SCF process. In addition, the solutions to the models were only obtained for successive generation times or doubling times. Liou et al. are currently working on a forthcoming communication that will deal with the coupling of the population balance equation to a substrate balance equation, but nevertheless there is a strong need to develop additional robust numerical techniques that efficiently capture the sharp spatial fronts and the temporal discontinuities inherent in the mathematical simulation of the SCF process.

Correspondence concerning this article should be addressed to A. D. Rey.

The SCF model consists of a nonlinear, partial-integro differential equation coupled to two nonlinear differential equations. The model is a segregated, structured cell-mass population-balance model, and is given as:

$$\frac{\partial W(t,m)}{\partial t}+\frac{\partial\left[r(m,C_s)W(t,m)\right]}{\partial m} = 2\int_m^\infty \Gamma'(m',C_s)W(t,m')\,p(m,m')\,dm' - \Gamma'(m,C_s)W(t,m) - \sum_{j=1}^{\infty} fW(t,m)\,\delta\left(t-t_{\min O_2,j}\right) \tag{1}$$

$$\frac{dC_s}{dt} = -\int_0^\infty Y_{s/x}r'(m,C_s)W(t,m)\,dm + \sum_{j=1}^{\infty}\left[f\delta\left(t-t_{\min O_2,j}\right)\left(C_s^0-C_s\right)\right] \tag{2}$$

$$\frac{dC_O}{dt} = k_L a\left(C_O^*-C_O\right)-\int_0^\infty Y_{O/x}r'(m,C_s)W(t,m)\,dm + \sum_{j=1}^{\infty}\left[f\delta\left(t-t_{\min O_2,j}\right)\left(C_O^0-C_O\right)\right] \tag{3}$$

$$N=\int_0^\infty W(t,m)\,dm \tag{4}$$

$$C=\int_0^\infty mW(t,m)\,dm. \tag{5}$$

For clarity, the symbols used in this model are defined in the Notation section at the end of this article. The total cell number concentration, N, and the biomass concentration, C, are given by Eqs. 4 and 5, respectively. The model must be solved for the cell-mass distribution, $W(t,m)$, the substrate concentration, $C_s(t)$, and the dissolved oxygen concentration, $C_O(t)$, as a function of time. The single-cell growth rate, $r(m,C_s)$, is expressed as the difference between two terms:

$$r(m,C_s)=r'(m,C_s)-r''(m), \tag{6}$$

where $r'(m,C_s)$ is the rate of cell-mass uptake and $r''(m)$ is the rate of cell mass released. The rate of cell-mass uptake is assumed to follow first-order kinetics and is expressed as

$$r'(m,C_s)=\frac{\mu' C_s}{K_s+C_s}\left(\frac{2m}{R\rho}\right). \tag{7}$$

The rate of cell mass released is given as

$$r''(m)=\mu_c m. \tag{8}$$

The transition probability function for cell division, $\Gamma'(m,C_s)$, is written as

$$\Gamma'(m,C_s)=\frac{2e^{-[(m-m_c)/\epsilon]^2}r(m,C_s)}{\epsilon\sqrt{\pi}\,\mathrm{erfc}\left(\frac{m-m_c}{\epsilon}\right)}, \tag{9}$$

and the density of daughter cell mass distribution, $p(m,m')$, is expressed as

$$p(m,m')=\frac{e^{\{[m-(1/2\,m')]/\epsilon'\}^2}}{\epsilon'\sqrt{\pi}\,\mathrm{erf}\left(\frac{m'}{2\epsilon'}\right)}. \tag{10}$$

In this model, cell division occurs when the organisms approach a critical cell mass, m_c. The functionality of the critical division mass is such that the critical division mass decreases with decreasing substrate concentration. This relationship, along with the detailed formulation of the SCF model, are further discussed by Godin et al. (1998).

The boundary condition on the solution of Eq. 1 is given as

$$r(\infty,C_s)W(t,\infty)=0, \tag{11}$$

which states that the convective flux vanishes as $m\to\infty$.

The numerical method developed here solves the microbial population balance for the SCF process using the Galerkin finite-element method (Finlayson, 1980; Lapidus and Pinder, 1982). The implicit predictor–corrector Euler scheme (Finlayson, 1980; Gerald, 1994) along with a variable time stepping scheme is used to integrate the microbial population model in time. The sections that follow discuss the application of these methods to solve the microbial population balance model for the SCF system.

Application of the Galerkin Finite-Element Method to the SCF Model

To solve the cell-mass population-balance equation (Eq. 1) for the cell-mass distribution, $W(t,m)$, the following trial solution is defined:

$$\hat{W}(t,m)=\sum_{j=1}^{N} w_j(t)\theta_j(m), \tag{12}$$

where $\hat{W}(t,m)$ is the trial solution for the cell mass distribution, $w_j(t)$ are unknown functions of time, $\theta_j(m)$ are known nearly orthogonal basis functions, and N is the number of nodes in the mesh spanning the cell-mass domain $0\le m\le m_{\max}$, where $m_{\max}$ is the upper cell-mass limit above which, for all practical purposes, no cells exist. By substituting this trial solution into Eq. 1, the residual R is defined as:

$$R=\frac{\partial\hat{W}(t,m)}{\partial t}+\frac{\partial\left[r(m,C_s)\hat{W}(t,m)\right]}{\partial m} -2\int_m^\infty \Gamma'(m',C_s)\hat{W}(t,m')\,p(m,m')\,dm' + \Gamma'(m,C_s)\hat{W}(t,m)+\sum_{j=1}^{\infty} f\hat{W}(t,m)\,\delta\left(t-t_{\min O_2,j}\right)\neq 0. \tag{13}$$

The residual is a measure of the error that occurred when the trial solution was substituted into the cell-mass population-balance equation. The problem lies in obtaining the

functions w_j that minimize the residual. This is done by setting the inner product of the residual and of a set of weighing functions equal to zero:

$$\int_0^{m_{\max}} R \cdot \phi_i \, dm = 0, \tag{14}$$

where ϕ_i are the weighing functions, and $m_{\max}$ is the upper cell-mass limit of the finite mesh defined such as to span the entire domain over which the cell-mass distribution has a nonzero solution. Applying the Galerkin method, the weighing functions were set equal to the basis function such that

$$\int_0^{m_{\max}} R \cdot \theta_i \, dm = 0; \qquad i = 1, 2, 3, \ldots, N. \tag{15}$$

In addition, the population balance equation is also coupled to the limiting substrate balance. In this simulation, a single limiting substrate is assumed, although the solution to the model could be obtained for more than one substrate. Also, the oxygen balance equation is coupled to both the population balance equation and the limiting substrate equation. Therefore, a total of $N+2$ unknowns must be solved in $N+2$ equations. Rewriting this system of equations in vector notation yields:

$$F(y) = 0, \tag{16}$$

where

$$F(y) = \begin{bmatrix} f_1(y) \\ f_2(y) \\ f_3(y) \\ \vdots \\ f_N(y) \\ S(y) \\ DO(y) \end{bmatrix}, \qquad y = \begin{bmatrix} w_1 \\ w_2 \\ w_3 \\ \vdots \\ w_N \\ C_s \\ C_{\mathrm{O}} \end{bmatrix}, \tag{17}$$

$$\begin{aligned} f_i = \int_0^{m_{\max}} R \cdot \theta_i \, dm &= \int_0^{m_{\max}} \frac{\partial \hat{W}(t,m)}{\partial t} \theta_i \, dm \\ &+ \int_0^{m_{\max}} \frac{\partial \left[r(m, C_s) \hat{W}(t,m) \right]}{\partial m} \theta_i \, dm \\ &- \int_0^{m_{\max}} \left(2 \int_m^{\infty} \Gamma'(m', C_s) \hat{W}(t, m') p(m, m') \, dm' \right) \theta_i \, dm \\ &+ \int_0^{m_{\max}} \Gamma'(m, C_s) \hat{W}(t,m) \theta_i \, dm \\ &+ \int_0^{m_{\max}} \sum_{j=1}^{\infty} \left[f \hat{W}(t,m) \delta\left(t - t_{\mathrm{minO}_2, j}\right) \right] \theta_i \, dm = 0 \end{aligned}$$

$$i = 1, 2, \ldots, N, \tag{18}$$

$$S = \frac{dC_s}{dt} + \int_0^{m_{\max}} Y_{s/x} r'(m, C_s) \hat{W}(t,m) \, dm - \sum_{j=1}^{\infty} \left[f \delta\left(t - t_{\mathrm{minO}_2, j}\right) \left(C_s^0 - C_s\right) \right] = 0, \tag{19}$$

and

$$DO = \frac{dC_{\mathrm{O}}}{dt} - k_L a (C_{\mathrm{O}}^* - C_{\mathrm{O}}) + \int_0^{m_{\max}} Y_{\mathrm{O}/x} r'(m, C_s) \hat{W}(t,m) \, dm - \sum_{j=1}^{\infty} \left[f \delta\left(t - t_{\mathrm{minO}_2, j}\right) \left(C_{\mathrm{O}}^0 - C_{\mathrm{O}}\right) \right] = 0. \tag{20}$$

The solution vector y of Eq. 16 is solved using the Newton-Raphson iteration scheme. For the vector equation, this scheme may be written as

$$F\left(y^{k+1}\right) = F\left(y^k\right) + \bar{J} \cdot \left(y^{k+1} - y^k\right) = 0, \tag{21}$$

where k is the iteration index, and $\bar{J}$ is the Jacobian matrix:

$$J_{ij} = \frac{\partial F_i}{\partial y_j}. \tag{22}$$

This iterative scheme can be rewritten as

$$y^{k+1} = y^k - J_{ij}^{-1} F\left(y^k\right). \tag{23}$$

With each iteration, the vector y^{k+1} converges quadratically toward its true value. The iteration is carried out until the difference between successive solutions reaches a value below a user-specified tolerance.

Chapeau basis functions (Lapidus and Pinder, 1982), that is to say the function θ_j in Eqs. 12 and 15, were used to solve the cell-mass population-balance equation. These functions are linear and nearly orthogonal in that they ''hardly'' overlap. Consequently, when evaluating the integrals in f_i, the integration limits may be reduced to values covering the range where θ_i is nonzero. In addition, over each element of the mesh, there are only two contributions from the basis functions. Therefore the Jacobian matrix, $\bar{J}$, is a banded matrix. This reduces the likelihood of having to solve ill-conditioned matrices. The integrals were solved using a 3-point Gaussian quadrature method. The boundary condition is implemented by applying the condition given by Eq. 11 at the node where m is equal to $m_{\max}$.

Predictor–Corrector Euler Scheme

The solution to the $N+2$ equations just discussed must be found as a function of time. This is accomplished using the implicit predictor–corrector Euler scheme (Finlayson, 1980). This numerical method consists of two steps. The first is an explicit predictor step in which a solution is approximated from earlier, known solutions.

Using the notation developed in the previous section, the predictor step can be written as

$$y_{n+1}^p = y_n + \Delta t_{n+1} \left(\frac{y_n - y_{n-1}}{\Delta t_n} \right), \tag{24}$$

where y_{n+1}^p is the predicted value of the vector y; y_n to y_{n-1} are the known values of the vector at time t_n and t_{n-1}, respectively; Δt_{n+1} and Δt_n are the user specified time step

from t_n to t_{n+1} and t_{n-1} to t_n, respectively; and n is the solution index. The term in the parentheses is the first-order difference approximation of the first time derivative of y at time t_n.

The second step consists of an implicit procedure that corrects the predicted value y^p_{n+1} to yield a more accurate solution for y_{n+1}. This procedure uses the predicted solution y^p_{n+1} to estimate the time derivatives at t_{n+1}:

$$\frac{\partial y_i}{\partial t} = \frac{y^p_{i,n+1} - y_{i,n}}{\Delta t_{n+1}}. \tag{25}$$

This approximation, along with the predicted value y^p_{n+1} is then resubstituted back into Eq. 16 and the Newton-Raphson iteration scheme is used to find the corrected solution y^c_{n+1} at time t_{n+1}. If the absolute difference between the predicted and corrected values is greater than a user-specified tolerance, in the case of this work $|y^p_{n+1} - y^c_{n+1}| \geq 1 \times 10^{-8}$, the solution is rejected and the process is repeated with a smaller time step. If this difference is within the specified tolerance, the solution is accepted and the process is continued to find the next solution y_{n+2}. The time steps Δt_n were originally specified by the user, and were reduced by half if the solution did not converge within three iterations. Similarly, the time steps were multiplied by 1.2 if the solution converged in less than three iterations. This ensured that the stepping algorithm remained efficient if the conditions were such that larger time steps could be used.

To verify the solution scheme, the method was used to solve the chemostat and batch models discussed by Subramanian and Ramkrishna (Ramkrishna, 1971; Subramanian and Ramkrishna, 1971). The solution to these models obtained using the solution scheme discussed here was then compared to the solution obtained by Subramanian and Ramkrishna. These results are discussed in Godin et al. (1998).

Solution of the SCF Model

The parameter values used in these simulations are given in Table 1. Figures 1 and 2 are the numerical solution to the model of the SCF process after it has reached its stable periodic state. Figure 1 shows the biomass concentration (upper plot), the limiting substrate concentration (middle plot), and the dissolved oxygen concentration (bottom plot) as a function of time. Figure 2 depicts the cell-number concentration as a function of time, with the total cell number staying constant for the initial time period within each cycle. Figures 1 and 2 show the effect of cycling on the growth curves. The sudden emptying and refilling of the reactor volume introduces discontinuities in time. These figures demonstrate that

Table 1. Parameter Values Used in the Simulations of the SCF Process

Parameters*	Values
C_O^0	0.0371 g/L
C_O^*	0.0371 g/L
C_s^0	0.6246 g/L
f	1/2
$k_L a$	145.2 h^{-1}
K_s	0.01 g/L
R	5×10^{-5} cm
$Y_{s/x}$	1.31
$Y_{O/x}$	5.45
ϵ	1.061×10^{-13} g
ϵ'	5×10^{-14} g
μ'	1.515×10^{-5} g/(cm^2·h)
μ_c	0 h^{-1}
ρ	1.01 g/cm^3

*The symbols are defined in the Notation section.

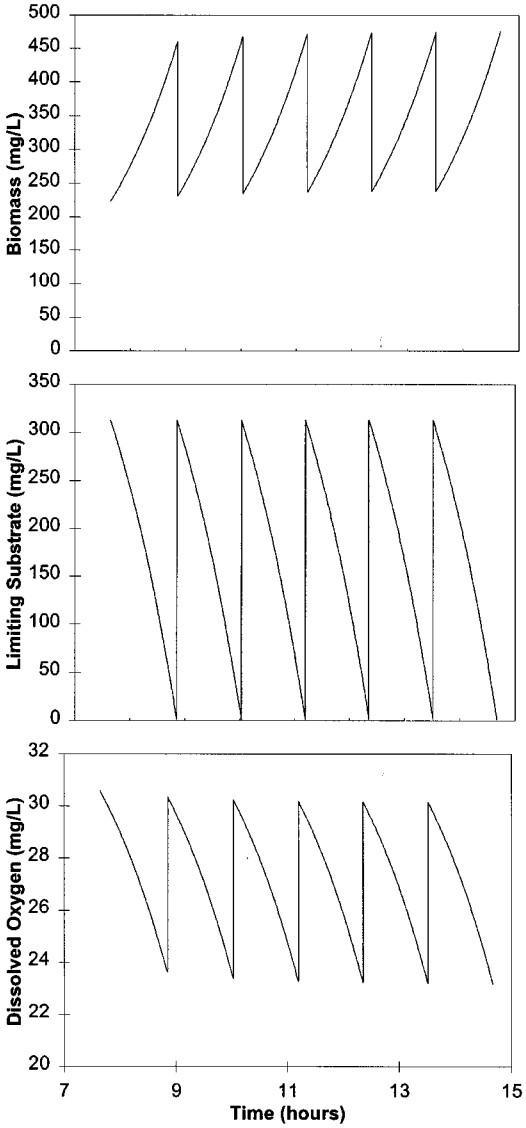

Figure 1. Simulation of biomass concentration, C (upper), limiting substrate concentration, C_s (middle), and DO concentration, C_O (bottom), as a function of time for the SCF system.

The sharp discontinuities represent the cycling of the reactor in which half of the volume is replaced by fresh medium. The control of cycling is achieved by monitoring a growth-associated parameter and allowing the reactor to cycle when an extremum is detected. Despite the sharp discontinuities, the numerical solution does not display any oscillations or overshoot.

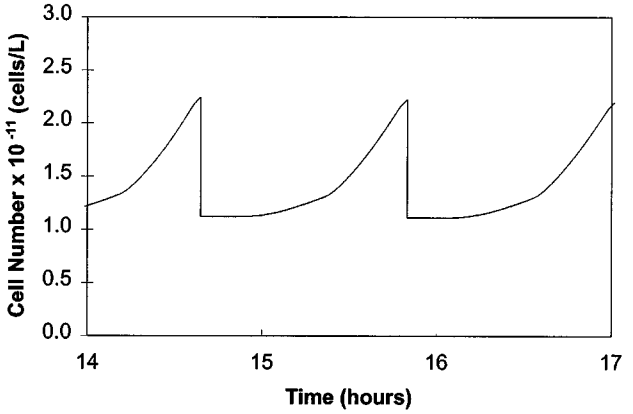

Figure 2. Simulation for the cell number profile, *N*, as a function of time for the SCF system.

The cell number profile is characterized by a constant total cell number concentration during the early part of each cycle, followed by a sudden increase in cell number toward the end of the cycle. The sudden drop in cell number corresponds to cycling of the reactor. Again, no oscillations or overshoot is observed in the numerical solution.

the numerical stepping scheme was able to capture these sharp trends without overshoot or oscillations. Figure 3 shows the time steps as a function of time. The time steps decrease progressively throughout each cycle. This is explained by the fact that as the cell population increases in the reactor, the rate of change of the growth-associated curves also increase. In order to maintain accurate numerical solutions, the time steps are reduced accordingly. Immediately after the reactor has cycled, the time step is reduced even further to a value close to zero, since the input to the system is singular at this point. Once solutions are found for two consecutive times

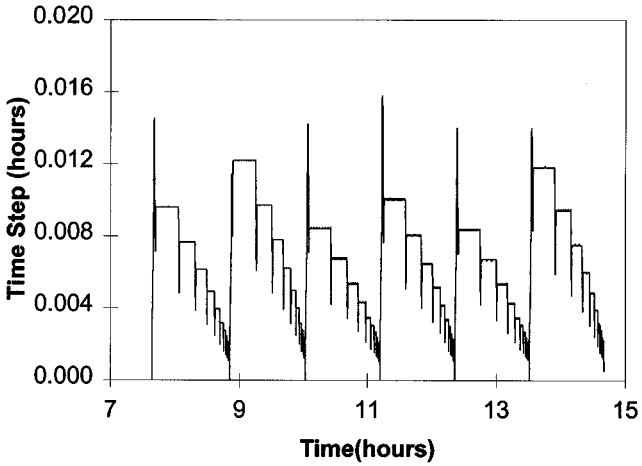

Figure 3. Integration time steps as a function of time obtained using the adaptive predictor–corrector Euler scheme.

The time steps, Δt, are controlled by the algorithm so that a user-specified accuracy is always maintained. Note that after each cycle, the time steps increase rapidly initially, then progressively decrease as a new cycle is approached, at which point it is nearly zero since the input to the system is singular.

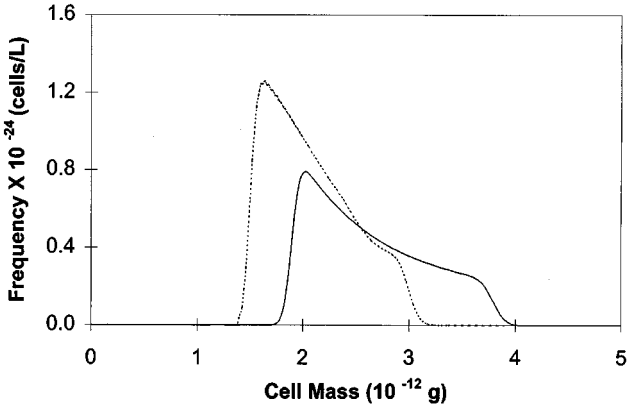

Figure 4. Simulation for the cell mass distribution prior to doubling of the organisms (solid line) and immediately after cycling (dashed line) of the SCF system.

The figure depicts the narrower cell mass distributions associated with synchronized cell populations. The cell mass distribution profile takes on a sharper profile immediately after cycling and becomes smoother as the distribution propagates along the cell mass space. The initial propagation without cellular division results in the constant total cell number observed at the beginning of each cycle. The Galerkin finite-element method is able to capture the sharp spatial changes by using localized basis functions.

after cycling, the time steps immediately increase to maintain an efficient progression in time. This is seen as the large steplike increases in the time steps. It is worth noticing that the time steps exhibit frequent overshoot when changing to new values. The time steps eventually stabilize over short intervals when the time steps are adequate to fulfill the user-specified conditions of accuracy and efficiency. Therefore the stepping scheme allows for the user to specify the accuracy required while maintaining an efficient numerical scheme.

Figure 4 shows the cell-mass distribution of the system prior to the doubling of the organisms (solid line), and immediately after cycling (dashed line). The figure depicts the narrower cell-mass distributions associated with synchronized cell populations. The younger cells also take on a sharper profile immediately after cycling. The distribution becomes smoother as the distribution propagates along the cell-mass space. The initial propagation without cellular division results in the constant total cell number observed at the beginning of each cycle. The use of localized basis functions allows for this front profile to be captured without oscillations or overshoot. This method reduced the number of nodes required for these simulations. In the present case, 81 nodes were used for this simulation, with the distribution of nodes accommodated such that they were concentrated in the space spanned by the cell-mass distribution $W(m, t)$. In particular, half of the nodes were evenly distributed between the cell-mass values of 1.151×10^{-12} g and 1.951×10^{-12} g with a spacing of 0.0195 g, thereby capturing the sharp features over this region. The solution scheme was very robust and converged quickly, usually within three iterations. Using localized basis functions also reduced the problem of inverting the Jacobian matrix to the inversion of a banded matrix, therefore reducing the likelihood of encountering singular matrices. This would also al-

low for an increase in the number of nodes, if this were required to appropriately capture the numerical solution.

Conclusion

A numerical solution scheme using the Galerkin finite-element method, along with a predictor–corrector Euler scheme, was developed and applied to solve the population balance model of a real fermentation system known as self-cycling fermentation. The model consisted of a nonlinear, partial-integro differential equation coupled to two time-dependent, nonlinear differential equations. Due to the synchronized nature of this cell culture, the solution to the model had sharper cell-mass distributions when compared to nonsynchronized cell cultures. Furthermore discontinuities in time were present in the growth curves. An accurate solution was found and the method proved to be robust and efficient. An adaptive time-stepping scheme was used to capture the time discontinuities without introducing oscillations or overshoot, while maintaining a maximum efficiency between cycling events, thereby reducing computing time. The localized basis functions were able to capture the sharp cell-mass distributions associated with synchronized cell culture while reducing the possibility of generating ill-conditioned matrices. Although this model was solved for a single substrate, the solution scheme could be modified to include multiple substrates. In addition, the same approach could be used to solve population-balance models with more than one spatial dimension, as well as population balance models dealing with different processes in other fields of study.

Notation

C_O^0 = concentration of dissolved oxygen in the feed stream, g/L
C_O^* = concentration of dissolved oxygen at saturation, g/L
C_s^0 = concentration of limiting substrate in the feed stream, g/L
f = emptying/fill fraction
j = cycle number
$k_L a$ = volumetric oxygen transfer coefficient, h^{-1}
K_s = saturation constant, g/L
m' = cell mass, g
R = radius of rod-shaped cell, cm
$t_{\min O_2, j}$ = time at the DO minimum of cycle j, h
$Y_{O/x}$ = fraction of oxygen in the mass taken up by the cell, g oxygen/g cell mass
$Y_{s/x}$ = fraction of limiting substrate in the mass taken up by the cell, g limiting substrate/g cell mass
$\delta(t)$ = delta Dirac function
ϵ = measure of spread in division mass distribution, g
ϵ' = measure of spread in daughter cell-mass distribution, g
μ' = maximum mass flux, g/(cm^2·h)
μ_c = specific mass release rate, g/(cm^2·h)
ρ = density of cells, g/cm^3

Literature Cited

Brown, W. A., and D. G. Cooper, "Self-Cycling Fermentation Applied to *Acinetobacter calcoaceticus* RAG-1," *Appl. Environ. Microbiol.*, **57**(10), 2901 (1991).

Brown, W. A., and D. G. Cooper, "Hydrocarbon Degradation by *Acinetobacter calcoaceticus* RAG-1 Using the Self-Cycling Fermentation Technique," *Biotech. Bioeng.*, **40**, 797 (1992).

Finlayson, B. A., *Nonlinear Analysis in Chemical Engineering, Chemical Engineering Series*, McGraw-Hill, New York (1980).

Fletcher, C. A. J., *Computational Galerkin Methods*, Springer-Verlag, New York (1984).

Gerald, C. F., *Applied Numerical Analysis*, Addison-Wesley, New York (1994).

Godin, F. B., D. G. Cooper, and A. D. Rey, "Development and Solution of a Cell Mass Population Balance Model Applied to the SCF Process," *Chem. Eng. Sci.*, **54**, 565 (1999).

Himmelblau, D. M., and K. B. Bischoff, *Process Analysis and Simulation: Deterministic Systems*, Wiley, New York (1968).

Hughes, S. M., and D. G. Cooper, "Biodegradation of Phenol Using the Self-Cycling Fermentation (SCF) Technique," *Biotech. Bioeng.*, **51**, 112 (1996).

Lapidus, L., and G. F. Pinder, *Numerical Solution of Partial Differential Equations in Science and Engineering*, Wiley, Toronto, Canada (1982).

Liou, J. J., F. Srienc, and A. G. Fredrickson, "Solutions of Population Balance Models Based on a Successive Generations Approach," *Chem. Eng. Sci.*, **52**, 1529 (1997).

McCaffrey, W. C., and D. G. Cooper, "Sophorolipids Production by *Candida bombicola* Using Self-Cycling Fermentation," *J. Ferment. Bioeng.*, **79**, 146 (1995).

Ramkrishna, D., "Solution of Population Balance Equations," *Chem. Eng. Sci.*, **26**, 1134 (1971).

Ramkrishna, D., "The Status of Population Balances," *Rev. Chem. Eng.*, **3**(1), 49 (1985).

Sarkis, B., and D. G. Cooper, "Biodegradation of Aromatic Compounds in a Self-Cycling Fermentor (SCF)," *Can. J. Chem. Eng.*, **72**, 874 (1994).

Sheppard, J. D., and D. G. Cooper, "Development of Computerized Feedback Control for the Continuous Phasing of *Bacillus subtilis*," *Biotech. Bioeng.*, **36**, 539 (1990a).

Sheppard, J. D., and D. G. Cooper, "The Response of *Bacillus subtilis* ATCC 21332 to Manganese During Continuous-Phased Growth," *Appl. Microbiol. Biotechnol.*, **35**, 72 (1990b).

Subramanian, G., and D. Ramkrishna, "On the Solution of Statistical Models of Cell Populations," *Math. Biosci.*, **10**, 1 (1971).

van Walsum, G. P., and D. G. Cooper, "Self-Cycling Fermentation in a Stirred Tank Reactor," *Biotech. Bioeng.*, **42**, 1175 (1993).

Wentworth, S. D., and D. G. Cooper, "Self-Cycling Fermentation of a Citric Acid Producing Stain of *Candida lipolytica*," *J. Ferment. Bioeng.*, **81**, 400 (1996).

Zenaitis, M. G., and D. G. Cooper, "Antibiotic Production by *Streptomyces aureofaciens* Using Self-Cycling Fermentation," *Biotech. Bioeng.*, **44**, 1331 (1994).

Manuscript received Oct. 19, 1998, and revision received Mar. 24, 1999.